Available online at www.sciencedirect.com
SCIENCE DIRECT®
Physica E 29 (2005) 469–474
PHYSICA E
www.elsevier.com/locate/physe

Magneto-optical spectroscopy of carbon nanotubes

S. Zaric[a], G.N. Ostojic[a], J. Shaver[a], J. Kono[a,*], X. Wei[b], M. Furis[c], S.A. Crooker[c], O. Portugall[d], P.H. Frings[d], G.L.J.A. Rikken[d], V.C. Moore[e], R.H. Hauge[e], R.E. Smalley[e]

[a]*Department of Electrical and Computer Engineering, Rice University, MS-366, 6100 Main St., Houston, TX 77005, USA*
[b]*National High Magnetic Field Laboratory, 1800 E. Paul Dirac Drive, Tallahassee, FL 32310, USA*
[c]*Optics and Laser Operations, National High Magnetic Field Laboratory, Mail Stop E536, Los Alamos, NM 87545, USA*
[d]*Laboratoire National des Champs Magnétiques Pulsés, 143 Avenue de Rangueil—BP 14245, Toulouse Cedex 4 F-31432, France*
[e]*Department of Chemistry, Rice University, P.O. Box 1892, MS-60, Houston, TX 77251, USA*

Available online 19 August 2005

Abstract

We review our recent optical experiments on single-walled carbon nanotubes in high magnetic fields. The data revealed magnetic-field-induced optical anisotropy as well as broadening, splittings, and shifts of interband absorption and photoluminescence peaks. Quantitative comparison with theoretical predictions based on the Aharonov–Bohm effect is presented.

PACS: 73.22.−f; 78.67.Ch; 75.75.+a

Keywords: Carbon nanotubes; Aharonov–Bohm effect; Photoluminescence; Absorption; Magnetic alignment

1. Introduction

The electronic structure of a single-walled carbon nanotube (SWNT) is influenced by a magnetic flux ϕ threading the tube. This is due to the modification in the circumferential boundary condition introduced by the Aharonov–Bohm (AB) phase. As a result, the band gaps of both semiconducting and metallic nanotubes are predicted [1,2] to oscillate as a function of a magnetic field with period $\phi_0 = e/h$, i.e., magnetic flux quantum. For a standard SWNT with a diameter of 1 nm, $\phi = \phi_0$ is achieved in an external field of ~6000 T applied parallel to the nanotube axis.

There have been electronic transport experiments on multiwalled [3–6] as well as (relatively large-diameter) single-walled [7,8] carbon nanotubes in magnetic fields. Although some of these

*Corresponding author. Tel.: +1 713 348 2209; fax: +1 713 348 5686.
E-mail address: kono@rice.edu (J. Kono).

1386-9477/$ - see front matter © 2005 Elsevier B.V. All rights reserved.
doi:10.1016/j.physe.2005.06.067

measurements exhibited AB phase-dependent conductance modulations, it is not clear how much of them come from the predicted band structure modifications (as opposed to magneto-conductance oscillations commonly seen in mesoscopic rings and cylinders at low temperature [9]). Optical spectroscopic studies in magnetic fields [10,11] are able to provide more direct and clear-cut evidence of the predictions.

States in the vicinity of the band gap of a semiconducting nanotube can be probed using light polarized parallel to the nanotube. The AB effect will cause the absorption peaks to split. The amount of splitting at low magnetic fields ($\phi < \phi_0/6$) is given by [1,2,12,13]

$$\Delta E_{AA} \equiv 6E_g\phi/\phi_0, \quad (1)$$

where E_g is the zero-field band gap. The inclusion of Coulomb interactions changes the above result in a diameter-dependent way [14]. For a nanotube with a diameter of 1 nm, the low-field rate of splitting is predicted to be enhanced by ~10%.

Another interesting consequence of the AB phase is the oscillating behavior of SWNT magnetic properties. At low fields $(\phi \ll \phi_0)$, molar magnetic susceptibilities parallel ($\chi_{\|}$) and perpendicular ($\chi_{\perp}$) to the nanotube axis satisfy $\chi_{\perp} < \chi_{\|}$ [15,16], which would cause both metallic and semiconducting nanotubes to align in external magnetic fields due to the aligning energy [17]

$$\Delta U = U(\pi/2) - U(0) = B^2N(\chi_{\|} - \chi_{\perp}) \quad (2)$$

for a SWNT with N moles of carbon atoms.

2. Experimental details

Liquid samples of SWNTs dissolved in water (or deuterium oxide) with 1% sodium dodecyl sulfate or sodium cholate hydrate surfactants were prepared as in Ref. [18]. Such samples contain SWNTs surrounded by surfactant molecules that prevent them from bundling with other nanotubes in the solution. This removal of the intertube coupling results in samples showing absorption and photoluminescence (PL) peaks that correspond to specific chiralities present in the sample [19].

Absorption, PL and photoluminescence excitation (PLE) spectroscopy measurements were performed in the Voigt geometry in external magnetic fields. Absorption was measured both using light polarized parallel and perpendicular to the applied field.

DC field measurements (up to 45 T) were performed using the National High Magnetic Field Laboratory's (NHMFL, Tallahassee, FL, USA) hybrid magnet and the pulsed field measurements were performed using pulsed magnets at NHMFL (Los Alamos, NM, USA) and Laboratoire National des Champs Magnétiques Pulsés (LNCMP, Toulouse, France).

All the measurements were done at room temperature.

3. Experimental results

Fig. 1(a) shows near-infrared absorption spectra for the two polarizations (solid and dashed lines) in magnetic fields ($\boldsymbol{B}$) up to 45 T, demonstrating field-induced optical anisotropy. Here, different peaks correspond to the near-band-edge interband transitions in semiconducting SWNTs with different chiralities. Absorption for the parallel polarization ($\boldsymbol{B}\|\boldsymbol{P}$) increases with $\boldsymbol{B}$ while absorption for the perpendicular polarization ($\boldsymbol{B}\perp\boldsymbol{P}$) decreases with $\boldsymbol{B}$. Furthermore, parallel absorption data show significant spectral changes at fields above 30 T. Each absorption peak becomes broader with $\boldsymbol{B}$ and some of the peaks split at the highest fields, as shown in Fig. 1(b). These changes are not visible in the perpendicular absorption data.

PLE spectra for a SWNT sample at 0 and 45 T are shown in Fig. 2. Here, PL intensity is plotted as a simultaneous function of excitation photon energy and emission photon energy. A CW Ti:Sapphire laser was used as the tunable excitation source. All PL peaks (corresponding to specific chiralities) shift to lower energies and undergo spectral changes as the magnetic field is increased to 45 T. The magnetic field dependence of these spectral changes can be seen in more detail in Fig. 3, which shows the magnetic field evolution of the PL spectrum in the near-infrared for one specific excitation energy (1.65 eV or 750 nm). The

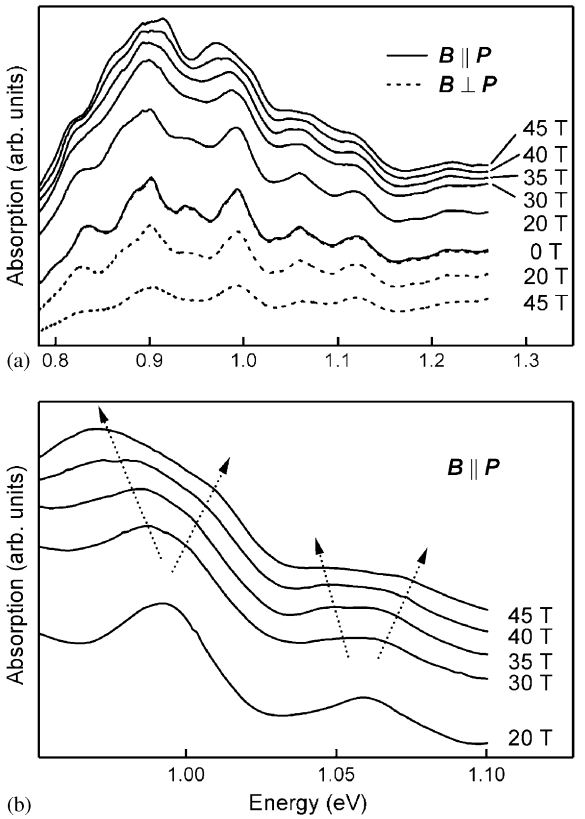

Fig. 1. Polarization-dependent absorption spectra for SWNTs suspended in aqueous solution at various magnetic fields up to 45 T taken in the Voigt geometry. (a) Absorption for light polarized parallel to B (solid line) and perpendicular to B (dashed line); (b) expanded detail from (a). All measurements were done at room temperature.

data up to 30 T mainly show peak broadening. At higher fields, shifts to lower energies become evident.

Finally, we measured polarization-dependent transmission in the Voigt geometry in pulsed magnetic fields up to 75 T, and some initial results are shown in Fig. 4. Fig. 4(a) shows a typical pulse profile of the ARMS magnet [20]. Fields are generated in a pulsed mode by simultaneously energizing two concentric coils utilizing the 14 MJ capacitor bank and a small 110 kJ "mobile" capacitor bank. Correspondingly, there is an extremely long pulse (~1 s) produced by the outer coil and then a short (~3 ms) impulse of the inner

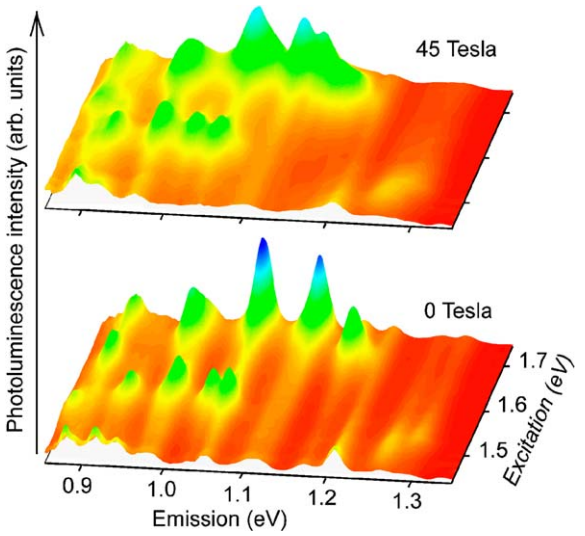

Fig. 2. Room temperature PLE spectra for a SWNT sample at (a) 45 T and (b) 0 T. A CW Ti:Sapphire laser was used for the excitation.

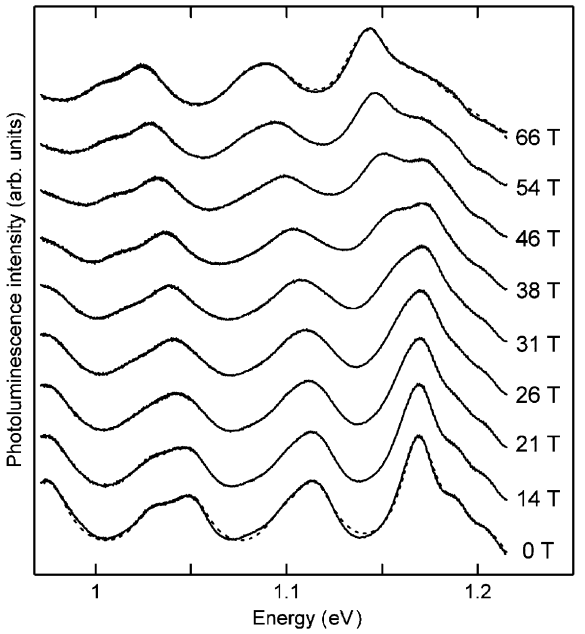

Fig. 3. Room temperature PL spectra for a SWNT sample at 0 T and at various fields during the falling edge of a magnetic pulse. The excitation was 750 nm using a CW Ti:Sapphire laser. Traces are offset for clarity. Dashed traces for the 0 and 66 T data represent the results of the fit and simulation, respectively, as described in the text.

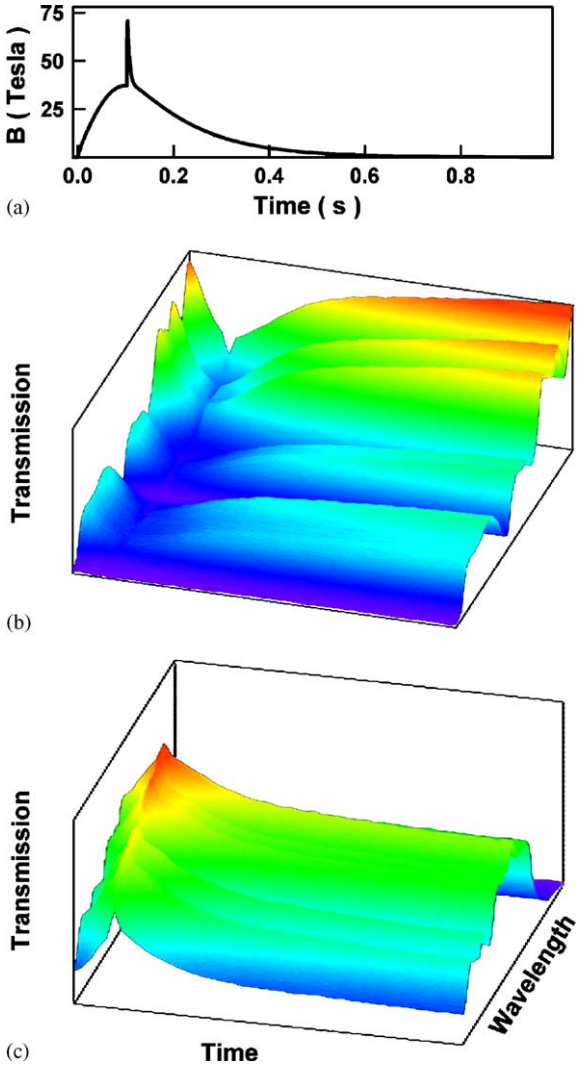

Fig. 4. Magneto-transmission data for SWNTs suspended in aqueous solution taken during the magnetic field pulse depicted in (a) for two polarizations: (b) parallel to $\boldsymbol{B}$ and (c) perpendicular to $\boldsymbol{B}$. Measurements were done at room temperature.

coil is produced at the top of the primary long pulse. Spectrally and temporally resolved transmission is shown for parallel and perpendicular polarizations in Figs. 4(b) and (c), respectively. It is seen that optical anisotropy clearly increases with the magnetic field, exhibiting even the influence of the short impulse by the inner coil in both polarizations.

4. Discussion

As expected from their predicted magnetic properties, the absorption data suggest that the nanotubes in the solution get aligned progressively better as the field is increased. The $\boldsymbol{B}\|\boldsymbol{P}$ absorption, which probes nanotubes close to the $\boldsymbol{B}$ direction, shows spectral changes suggesting the beginning of an absorption peak splitting while no spectral changes are observed for the $\boldsymbol{B}\perp\boldsymbol{P}$ case, which probes nanotubes mainly perpendicular to the $\boldsymbol{B}$ direction. This is also expected since nanotubes in the latter are not threaded by the magnetic flux.

The PL spectral changes depicted in Figs. 2 and 3 can be understood in terms of magnetic alignment of the nanotubes and the predicted changes of the nanotube electronic structure due to the threading magnetic flux [10,11]. At lower fields, because the alignment is still small, the measured PL spectrum represents the averaged PL of the nanotubes lying in a wide range of angles θ with respect to the external magnetic field $\boldsymbol{B}$. Furthermore, when the alignment is small, a nanotube pointing in any direction (defined by θ and the azimuthal angle φ) is approximately equally probable. After integrating the probability over the azimuthal angle, we arrive at the conclusion that the probability density of finding a nanotube at an angle θ is proportional to $\sin\theta$, thus it is more probable to find a nanotube at higher angles with respect to $\boldsymbol{B}$. These nanotubes are threaded with a relatively small flux, which explains why the PL peaks do not move at smaller fields. As the field is increased, the angle distribution moves towards smaller angles and the PL peak shifts become more evident.

Quantitative analysis of PL spectrum changes with $\boldsymbol{B}$ is based on Eqs. (1) and (2). Using Eq. (2) and Maxwell–Boltzman statistics, the probability density that a nanotube is at angle θ with respect to $\boldsymbol{B}$ can be written as [17]

$$\frac{\mathrm{d}P(\theta)}{\mathrm{d}\theta} = \frac{\exp(-u^2 \sin^2\theta)\sin\theta}{\int_0^{\pi/2}\exp(-u^2\sin^2\theta)\sin\theta\,\mathrm{d}\theta}, \tag{3}$$

where

$$u \equiv \{B^2 N(\chi_\| - \chi_\perp)/k_\mathrm{B}T\}^{1/2}, \tag{4}$$

where k_B is the Boltzmann constant and T is the temperature.

Zero-field PL data can be fitted using Lorentzians, where different peaks correspond to different chiralities present in the sample. By adjusting the u values for different peaks along with the rate of splitting, the 66 T PL data can be successfully reproduced (dashed lines in Fig. 3). This treatment gives us values for the splitting rates as ~0.9 meV/T [10], which is comparable with the theory [1–5].

The obtained values for u can be used to estimate $\chi_{\parallel}-\chi_{\perp}$ [11]. The length distribution of the nanotubes in the sample was measured using an atomic force microscope, which yielded estimates for the number of moles N for each nanotube. Then, using Eq. (4), $\chi_{\parallel}-\chi_{\perp}$ can be estimated. The obtained value 1.4×10^{-5} emu/mol is in agreement with the existing theoretical results [15,16].

In order to see clearer splittings in absorption, magnetic fields higher than 45 T must be used. This can be accomplished by using pulsed magnetic fields. Given the importance of the alignment in the measured data, a crucial question is whether the time of the applied pulse will allow nanotubes to align. The absorption data in Fig. 4 demonstrates that even millisecond pulses will still cause alignment. Absorption spectra up to 75 T, showing such clear splittings, have already been obtained and analyzed. These results will be described elsewhere [21].

5. Summary

We have performed magneto-optical studies of individualized single-walled carbon nanotubes in aqueous solution in high DC and pulsed high magnetic fields. We observed magnetic-field-induced spectral changes in photoluminescence and absorption, which are in agreement with predicted spectral changes due to the Aharonov–Bohm phase and the magnetic alignment of nanotubes. Quantitative analysis of the PL data also yielded the magnetic susceptibility value $\chi_{\parallel}-\chi_{\perp}$.

Acknowledgements

This work was supported by the Robert A. Welch Foundation (no. C-1509), the Texas Advanced Technology Program (no. 003604-0001-2001), and the National Science Foundation (no. DMR-0134058). We thank H.U. Mueller and M. von Ortenberg for the use of their InGaAs detector. A portion of this work was performed at the National High Magnetic Field Laboratory, which is supported by NSF Cooperative Agreement no. DMR-0084173 and by the State of Florida.

References

[1] H. Ajiki, T. Ando, J. Phys. Soc. Japan 62 (1993) 1255.
[2] H. Ajiki, T. Ando, Physica B 201 (1994) 349.
[3] A. Fujiwara, K. Tomiyama, H. Suematsu, M. Yumura, K. Uchida, Phys. Rev. B 60 (1999) 13492.
[4] A. Bachtold, C. Strunk, J.-P. Salvetat, J.-M. Bonard, L. Forro, T. Nussbaumer, C. Schonenberger, Nature 397 (1999) 673.
[5] J.-O. Lee, J.-R. Kim, J.-J. Kim, J. Kim, N. Kim, J.W. Park, K.-H. Yoo, Solid State Commun. 115 (2000) 467.
[6] U.C. Coscun, T.-C. Wei, S. Vishveshwara, P.M. Goldbart, A. Bezryadin, Science 304 (2004) 1132.
[7] E.D. Minot, Y. Yaish, V. Sazonova, P.L. McEuen, Nature 428 (2004) 536.
[8] J. Cao, Q. Wang, M. Rolandi, H. Dai, Phys. Rev. Lett. 93 (2004) 216803.
[9] A.G. Aronov, Y.V. Sharvin, Rev. Mod. Phys. 59 (1987) 755.
[10] S. Zaric, G.N. Ostojic, J. Kono, J. Shaver, V.C. Moore, M.S. Strano, R.H. Hauge, R.E. Smalley, X. Wei, Science 304 (2004) 1129.
[11] S. Zaric, G.N. Ostojic, J. Kono, J. Shaver, V.C. Moore, M.S. Strano, R.H. Hauge, R.E. Smalley, X. Wei, Nano Lett. 4 (2004) 2219.
[12] S. Roche, G. Dresselhaus, M.S. Dresselhaus, R. Saito, Phys. Rev. B 62 (2000) 16092.
[13] F.L. Shyu, C.P. Chang, R.B. Chen, C.W. Chiu, M.F. Lin, Phys. Rev. B 67 (2003) 045405.
[14] T. Ando, J. Phys. Soc. Japan 73 (2004) 3351.
[15] H. Ajiki, T. Ando, J. Phys. Soc. Japan 62 (1993) 2470; H. Ajiki, T. Ando, J. Phys. Soc. Japan 63 (1994) 4267; H. Ajiki, T. Ando, J. Phys. Soc. Japan 64 (1995) 4382.
[16] J.P. Lu, Phys. Rev. Lett. 74 (1995) 1123.
[17] D.A. Walters, M.J. Casavant, X.C. Qin, C.B. Huffman, P.J. Boul, L.M. Ericson, E.H. Haroz, M.J. O'Connel, K. Smith, D.T. Colbert, R.E. Smalley, Chem. Phys. Lett. 338 (2001) 14.

[18] M.J. O'Connell, S.M. Bachilo, C.B. Huffman, V.C. Moore, M.S. Strano, E.H. Haroz, K.L. Rialon, P.J. Boul, W.H. Noon, C. Kittrell, J. Ma, R.H. Hauge, R.B. Weisman, R.E. Smalley, Science 297 (2002) 593.
[19] S.M. Bachilo, M.S. Strano, C. Kittrell, R.H. Hauge, R.E. Smalley, R.B. Weisman, Science 298 (2002) 2361.
[20] H. Jones, P.H. Frings, M. von Ortenberg, A. Lagutin, L.V. Bockstal, O. Portugall, F. Herlach, Physica B 346–347 (2004) 553.
[21] S. Zaric, G.N. Ostojic, J. Kono, O. Portugall, P.H. Frings, G.L.J.A. Rikken, S.A. Crooker, X. Wei, J. Shaver, R.H. Hauge, R.E. Smalley, submitted for publication.